Received: 17 May 2017 | Accepted: 21 June 2017

DOI: 10.1111/gcb.13819

PRIMARY RESEARCH ARTICLE

WILEY Global Change Biology

Effects of free air carbon dioxide enrichment (FACE) on nitrogen assimilation and growth of winter wheat under nitrate and ammonium fertilization

Markus Dier[1,2*] | Rieke Meinen[3*] | Martin Erbs[4] | Lena Kollhorst[1] | Christin-Kirsty Baillie[3] | David Kaufholdt[3] | Martin Kücke[5] | Hans-Joachim Weigel[1] | Christian Zörb[2] | Robert Hänsch[3] | Remy Manderscheid[1]

[1]Thünen Institute of Biodiversity, Braunschweig, Germany

[2]Institute of Crop Science, Quality of Plant Products, University of Hohenheim, Stuttgart, Germany

[3]Institute of Plant Biology, Technische Universität, Braunschweig, Germany

[4]Deutsche Agrarforschungsallianz (DAFA) German Agricultural Research Alliance, c/o Thünen Institute, Braunschweig, Germany

[5]Julius Kühn Institute, Institute of Crop & Soil Science, Braunschweig, Germany

Correspondence
Remy Manderscheid, Thünen Institute of Biodiversity, Braunschweig, Germany.
Email: remy.manderscheid@thuenen.de

Funding information
Deutsche Forschungsgemeinschaft, Grant/Award Number: MA 1736/5-1; German Science Foundation (DFG)

Abstract

A 2-year **F**ree **A**ir **C**O_2 **E**nrichment (FACE) experiment was conducted with winter wheat. It was investigated whether elevated atmospheric CO_2 concentration (e[CO_2]) inhibit nitrate assimilation and whether better growth and nitrogen acquisition under e[CO_2] can be achieved with an ammonium-based fertilization as it was observed in hydroponic culture with wheat. Under e[CO_2] a decrease in nitrate assimilation has been discussed as the cause for observed declines in protein concentration in C_3 cereals. Wheat was grown under ambient [CO_2] and e[CO_2] (600 ppm) with three levels (deficiency, optimal, and excessive) of nitrate-based fertilization (calcium ammonium nitrate; CAN) or with optimal ammonium-based fertilization. Ammonium fertilization was applied via injection of an ammonium solution into the soil in the 1st year and by surface application of urea combined with nitrification inhibitors (UNI) in the 2nd year. Results showed that ammonium-based fertilization was successfully achieved in the 2nd year with respect to nitrification control, as soil ammonium concentration was considerably higher over the growing season for UNI fertilized plots compared to optimal CAN plots. Also, stem nitrate concentration, flag leaf nitrate reductase activity, and transcript levels were lower in UNI fertilized plants compared to optimal CAN. Regarding the e[CO_2] effect on nitrate reductase activity and transcript levels, no alteration could be observed for any nitrogen fertilizer treatment. Flag leaf growth was stimulated under e[CO_2] leading to an enhanced nitrate reductase activity referred to m^2 ground area at late flowering being in line with a higher nitrogen acquisition under e[CO_2]. Moreover, nitrogen acquisition was considerably higher in nitrate fertilized plants compared to ammonium fertilized plants under e[CO_2]. Our results obtained under field conditions show that a change from nitrate- to ammonium-based fertilization will not lead to a better growth and nitrogen acquisition of winter wheat under future e[CO_2].

KEYWORDS
ammonium fertilization, climate change, free air CO_2 enrichment, N acquisition, nitrate assimilation, nitrate fertilization, nitrate reductase, *Triticum aestivum*

*Both authors contributed equally to this work.

1 | INTRODUCTION

Atmospheric carbon dioxide concentration ($[CO_2]$) is predicted to continuously rise from currently 400 ppm $[CO_2]$ up to a level of 790–1020 ppm by the end of this century (IPCC, 2013). C_3 cereals react to elevated CO_2 concentration ($e[CO_2]$) with an increase in (i) photosynthetic CO_2 fixation (Ainsworth & Long, 2005), (ii) above- and belowground biomass production (Ma et al., 2007; Pacholski, Manderscheid, & Weigel, 2015; Ziska, Morris, & Goins, 2004), and (iii) grain yield (Han et al., 2015; Weigel & Manderscheid, 2012). However, CO_2 stimulation effects are generally accompanied by a considerable decrease in nitrogen (N) concentrations of plant tissue (Ainsworth & Long, 2005; Cotrufo, Ineson, & Scott, 1998; Taub, Miller, & Allen, 2008). The possible mechanisms behind this decrease remain elusive but have been linked to an altered nitrate (NO_3^-) assimilation (Bloom, Burger, Rubio-Asensio, & Cousins, 2010; Pleijel & Uddling, 2012).

NO_3^- is the main N form taken up by cereals from agricultural soils (Andrews, Raven, & Lea, 2013). At low soil NO_3^- concentrations, NO_3^- is primarily assimilated in the roots, but with increasing soil NO_3^- concentration, the NO_3^- reduction is shifted toward the leaves (Andrews, Morton, Lieffering, & Bisset, 1992). Ammonium (NH_4^+) is another important N source for cereals, however, with lower uptake and assimilation compared to NO_3^- due to rapid nitrification in the soil which converts NH_4^+ into NO_3^- (Andrews et al., 2013; Subbarao et al., 2006). Nitrification occurs in two consecutive steps, whereby the first step is the reduction in NH_4^+ to nitrite (NO_2^-) that acidifies the soil solution triggered by bacteria from the *Nitrosomonas* genera and the second step is the reduction in NO_2^- to NO_3^- triggered by bacteria from the *Nitrobacter* genera. High nitrification rates occur at a neutral soil solution pH (Suzuki, Dular, & Kwok, 1974). As cereal NH_4^+ uptake acidifies the soil solution and NO_3^- uptake alkalifies it, nitrification is therefore decreased by NH_4^+ but stimulated by plant NO_3^- uptake. NH_4^+ is mainly assimilated in roots via the glutamine synthetase/glutamate synthase pathway and incorporated into amino acids. NO_3^- assimilation follows the same pathway, but requires two consecutive upstream reactions. The first one is the reduction in NO_3^- to NO_2^- catalyzed by the enzyme nitrate reductase (NR) in the cytoplasm. The second reaction is the reduction in NO_2^- to NH_4^+ via nitrite reductase inside the chloroplasts.

Recent evidence indicates that $e[CO_2]$ might interfere with NO_3^- assimilation by impeding NO_3^- and NO_2^- reduction in C_3 plants (Bloom, 2015a). For instance, it has been observed in wheat and *Arabidopsis thaliana* that $e[CO_2]$ lowered the incorporation of ^{15}N labeled NO_3^- into organic N compounds (Bloom et al., 2010) and decreased the NR activity (NRA) of wheat leaves (Bloom, Smart, Nguyen, & Searles, 2002). Reduced NO_3^- assimilation of C_3 plants is thought to be strongly linked to a lower photorespiration rate under $e[CO_2]$ (Bloom, 2015a; Rachmilevitch, Cousins, & Bloom, 2004) and a subsequent decreased supply of the reductant nicotinamide adenine dinucleotide (NADH) which powers the NO_3^- reduction (Bloom, 2015b). Photorespiration drives the malate transport from the chloroplast into the cytoplasm where it is oxidized to oxalacetic acid for the generation of NADH (Bloom, 2015b; Rachmilevitch et al., 2004). This "malate valve" represents an important player in the complex network between N and C metabolism and is involved in supplying energy for NR (Scheibe, 2004; Taniguchi & Miyake, 2012).

The process of photorespiration is favored by the oxygenase function of ribulose-1,5-bisphosphate carboxylase/oxygenase (RuBisCO) under ambient $[CO_2]$ and high temperatures. Because $e[CO_2]$ shifts the activity of RuBisCO toward CO_2 fixation at high temperatures, inhibition of NO_3^- assimilation by $e[CO_2]$ is thought to take place primarily at elevated temperatures (Bloom, 2015b; Jauregui et al., 2015). However, the oxidation of triose phosphates, derived from CO_2 fixation, might also increase NADH availability and is therefore an important energy source for NO_3^- assimilation (Foyer, Bloom, Queval, & Noctor, 2009; Kaiser, Kandlbinder, Stoimenova, & Glaab, 2000). Consequently, the inhibition of NO_3^- assimilation induced by $e[CO_2]$ as cited above is assumed to be the reason for a decrease in plant N and in particular declining leaf and cereal grain protein concentrations (Bloom, 2015a; Bloom et al., 2010). A decline in leaf protein could negatively affect animal feedstuff quality and hence animal production including changes in livestock grazing patterns (Sinclair et al., 2000). Furthermore, a reduction in cereal grain protein might decrease flour baking quality (Wieser, Manderscheid, Erbs, & Weigel, 2008) and, particularly, could exacerbate protein deficiency in developing countries (Myers et al., 2014). Therefore, food and feed qualities are predicted to be severely affected by $e[CO_2]$ if cereals are continuously fertilized with NO_3^--dominated N fertilizer regimens (Bloom et al., 2010). To prevent these adverse effects of $e[CO_2]$ on NO_3^- assimilation and its resulting negative consequences for crop growth and food as well as feed quality it has been proposed to use NH_4^+-based N fertilizers as an alternative. This recommendation is based on laboratory experiments in hydroponics under $e[CO_2]$ conditions where several C_3 species showed enhanced growth and N acquisition when they received NH_4^+ instead of NO_3^- as a sole N source (Bloom et al., 2002, 2012; Carlisle, Myers, Raboy, & Bloom, 2012).

Thus far, nearly all experiments investigating $e[CO_2]$ effects on crop NO_3^- assimilation were conducted in hydroponic cultures under laboratory conditions with a restricted rooting volume (Bloom et al., 2002, 2010, 2012). These restrictions are known to strongly alter $e[CO_2]$ responses on growth and N acquisition (Arp, 1991; Long, Ainsworth, Leakey, & Morgan, 2005), which limits the reliability of predictions of $e[CO_2]$ effects on N assimilation in field-grown cereals based on such experiments. While there is only one field experiment under free air CO_2 enrichment (FACE) where an inhibition of NO_3^- assimilation by $e[CO_2]$ has been shown (Bloom, Burger, Kimball, & Pinter, 2014), there are no FACE experiments where NO_3^--based fertilization has been compared directly with NH_4^+-based N fertilization under $e[CO_2]$.

To test whether $e[CO_2]$ decreases NO_3^- assimilation in the field, a 2-year FACE experiment was carried out with winter wheat (*Triticum aestivum*) supplied with three levels of a NO_3^- and one level of

an NH_4^+-based fertilization. The NH_4^+-based fertilization was applied in the 1st year by **C**ontrolled **U**ptake **L**ong **T**erm **A**mmonium **N**utrition (CULTAN) fertilization, a method where nitrification immune NH_4^+ depots are injected into the root space at the beginning of the growing season (Petersen, Hansen, & Sorensen, 2004; Wetselaar, Passioura, & Singh, 1972). However, it is still a matter of discussion whether nitrification is effectively inhibited with CULTAN (Deppe et al., 2016). Therefore, in the 2nd year a NH_4^+-based fertilization was carried out by applying N as urea combined with nitrification inhibitors directly into the soil. There, urea is quickly transformed to NH_4^+, but the nitrification inhibitors impede the first nitrification step (Subbarao et al., 2006) and additionally prevent toxic NO_2^- accumulation in the soil (Ma, Shan, & Yan, 2015). Based on a sound field trial with three different quantities of NO_3^--based fertilization (deficiency, optimal, and excessive) together with an optimal quantity of NH_4^+ based fertilization the following hypotheses were tested: (i) Does e[CO_2] inhibit leaf NO_3^- assimilation in the field by decreasing NR activity and thus influencing NR transcript levels? and (ii) Is there an intensified growth stimulation without a decline in N acquisition if plants take up N primarily in form of NH_4^+ instead of NO_3^-?

2 | MATERIALS AND METHODS

2.1 | Experimental design and crop management

The experiment was conducted on a field site (52°18′N, 10°26′E, 79 ma.s.l.) at the Thünen Institute in Braunschweig, Germany, in 2014 and 2015. The mean annual temperature is 9.1°C and the mean annual precipitation is 617 mm. The soil profile has a depth of about 60 cm (−30 cm Ap, −15 cm Al, −15 cm Bt, and >60–70 cm CII). The lower layers, in particular >70 cm, are characterized by a coarser soil texture (almost pure sand) and are structured by the succession of thin silt/clay layers. The soil in the plough horizon (0–40 cm) is a luvisol of loamy sand texture (69% sand, 24% silt, and 7% clay). Measuring of soil variables in each subplot (mean±*SD*; $n = 24$) in March 2015 resulted in a pH of 6.88 ± 0.39 and a carbon and nitrogen content of 1.00 ± 0.04% and 0.09 ± 0.00%, respectively. The lower (−1.5 MPa) and upper limits (−0.01 MPa soil water tension) of plant-available soil water are a volumetric soil water content of 5 and 23%, respectively. Altogether, the soil has low-to-intermediate fertility with a shallow rooting zone.

Winter wheat (*Triticum aestivum* L. variety "*Batis*") was grown at ambient [CO_2] of about 390 ppm and e[CO_2] of 600 ppm. The CO_2 treatments were carried out on circular plots with a diameter of 20 m, in which four subplots (3 m × 5 m) as N treatments were randomly established. Altogether, the experiment consisted of eight different CO_2 × N fertilization combinations, which were replicated three times. The CO_2 plots were placed at the same position each year.

CO_2 enrichment was carried out by a FACE system constructed according to the Brookhaven National Laboratory design (Lewin, Hendrey, & Kolber, 1992). CO_2 enrichment started at the four leaf stage on March the 31st in 2014 and at the three leaf stage on March the 12th in 2015. CO_2 enrichment took place during the daytime hours and was interrupted if wind speed exceeded 6 m/s or if air temperature fell below 5°C. The 1 min average [CO_2] was within the range of 600 ppm ± 10% for 95.6% and 95.7% for the operation time in 2014 and 2015, respectively. The average daytime [CO_2] at the ambient air plots was 394 ppm in 2014 and 392 ppm in 2015.

Winter wheat was sown at the end of October with a density of 380 kernels/m^2. Crop management measures were performed according to local farm practice with adequate nutrient supply and pesticide applications. N fertilizer was applied as summarized in Table 1. Three different NO_3^--based N fertilization regimes were implemented with calcium ammonium nitrate (CAN, 27% N) with a deficient (CAN40/ CAN35), an optimal (CAN180/ CAN200) and an excessive (CAN320/ CAN320) quantity for 2014 and 2015, respectively. The optimal level corresponds to the present common agricultural practice. For CULTAN fertilization in 2014 (CUL180), a water solution of ammonium sulfate (8% N) was manually injected into the soil in a depth of 7 cm with a density of 24 injection holes per m^2. For the combined urea (46.5% N) and nitrification inhibitors treatment in 2015 (UNI200) the commercial urea fertilizer Alzon M+ (SKW Stickstoffwerke Piesteritz, Germany) was applied, containing 1.4% nitrification inhibitors (dicyandiamide + triazole). Supplementary nitrification inhibitors (5% triazole + methylpyrazole) were applied on three other dates to control nitrification (April 29th, May 11th, and June 15th 2015). The used amounts were equivalent to the quantity of inhibitors contained in Alzon M+ for the application of 10, 35, and 40 kg N/ha, respectively. To prevent drought stress and nitrate leaching, soil water content was kept in the range of 50–90% of plant-available water content by manual irrigation. Figure 1 presents daily mean temperature, precipitation, and irrigation over the main

TABLE 1 N fertilizer treatments with application dates and quantities. CAN refers to fertilization with calcium ammonium nitrate, CUL to CULTAN fertilization, and UNI to the application of urea + nitrification inhibitors

2014							2015					
	Quantity (kg N/ha)							Quantity (kg N/ha)				
	Mar 17th	Mar 19th	Apr 14th	May 4th	June 2nd	Total		Mar 18th	Apr 28th	May 11th	June 11th	Total
Treatment							Treatment					
CAN40		20	20			40	CAN35	15	15		5	35
CAN180		70	35	35	40	180	CAN200	70	35	35	60	200
CAN320		120	60	60	80	320	CAN320	120	60	60	80	320
CUL180	180					180	UNI200	70	35	35	60	200

growing season. Average temperature of the main growing season (April–July) in 2014 (15.2°C) and in 2015 (14.0°C) was similar to the long-term mean (1980–2010: 14.1°C). For monitoring plant water supply, volumetric soil water content in the 40 cm soil profile was measured twice a week with time domain reflectometry (TDR) sensors.

2.2 | Determination of soil NO_3^--N and NH_4^+-N and stem NO_3^- concentration

For winter wheat growth at this site, it was found that 90% of the root biomass was located in the 0–30 cm soil profile (Pacholski et al., 2015). Therefore, soil samples from the 30 cm soil profile were taken on a weekly basis from CAN200- and UNI200-treated subplots in 2015. At each sampling, subsamples with approx. 40 g soil were taken from six random positions of each subplot and the subsamples were pooled for further analysis. Soil samples were extracted with $CaCl_2$ (0.01 M) and NO_3^--N and NH_4^+-N determinations were carried out photometrically with a Continuous-Flow Analyzer (Model SA3000/5000, Scalar, Netherlands).

Stems from 30 plants were randomly chosen from four destructive harvests (0.5 m^2 ground area) at early stem elongation, early heading, flowering, and milk-ripe stage. Stem NO_3^- concentration was determined according to Padgett and Leonard (1993) with some modifications. Stem material was ground to a fine powder in a rotor mill (Brabender, Duisburg, Germany) after drying at 105°C. For each sample, 50 mg stem material was mixed with 25 ml distilled water and incubated in a 45°C water bath for 4 hr. The extracts and water blanks were gravity filtered through Whatman No.1 filters and analyzed photometrically as described above.

2.3 | Flag leaf sampling for nitrate reductase activity and growth parameter determination

Flag leaves were sampled twice before flowering in 2014. In 2015 flag leaves were sampled before flowering and at late flowering. The sampling dates and the related environmental conditions are shown in Table 2. At each sampling 10 flag leaf blades were randomly selected from all experimental plots and N treatments, respectively. They were immediately frozen and ground to a fine powder in liquid N_2 for further analyses. In addition, 20 flag leaf blades were sampled to measure fresh weight, leaf area with a leaf area meter (Model LI-3100, LICOR, USA), and dry weight after drying at 105°C. With these data dry weight/fresh weight ratio, individual flag leaf area (FLA), individual flag leaf biomass, and specific flag leaf weight (SFLW) were calculated.

Flag leaf number (FLN) was derived from ear number counted in destructive plant harvest of 0.5 m^2 ground area at flowering and milk-ripe stage and of 1.8 m^2 ground area at grain maturity. Flag leaf biomass per m^2 ground area (FLB) was determined by multiplying individual flag leaf biomass with FLN. Flag leaf area index (FLAI) was calculated as the quotient from FLB and SFLW.

2.4 | Total canopy sampling and green area index determination of ear and residual leaves

Three destructive harvests were taken at early heading, flowering, and milk-ripe stage (0.5 m^2 ground area). Green area of leaf blades and ears was determined with a leaf area meter (Model LI-3100

TABLE 2 Dates of flag leaf sampling for NRA determination and environmental conditions during sampling. Values are indicated as daily average and for the hour of sampling. Samples were always taken at midday between 1 and 2 p.m.

	2014		2015	
Date	May 19th	May 22th	May 29th	June 15th
Daily mean temperature (°C)	14.4	22.8	13.2	13.5
Temperature at sampling (°C)	16.7	27.6	16.5	18.2
Daily mean irradiance (W/m^2)	214	290	223	322
Irradiance at sampling (W/m^2)	791	762	383	898

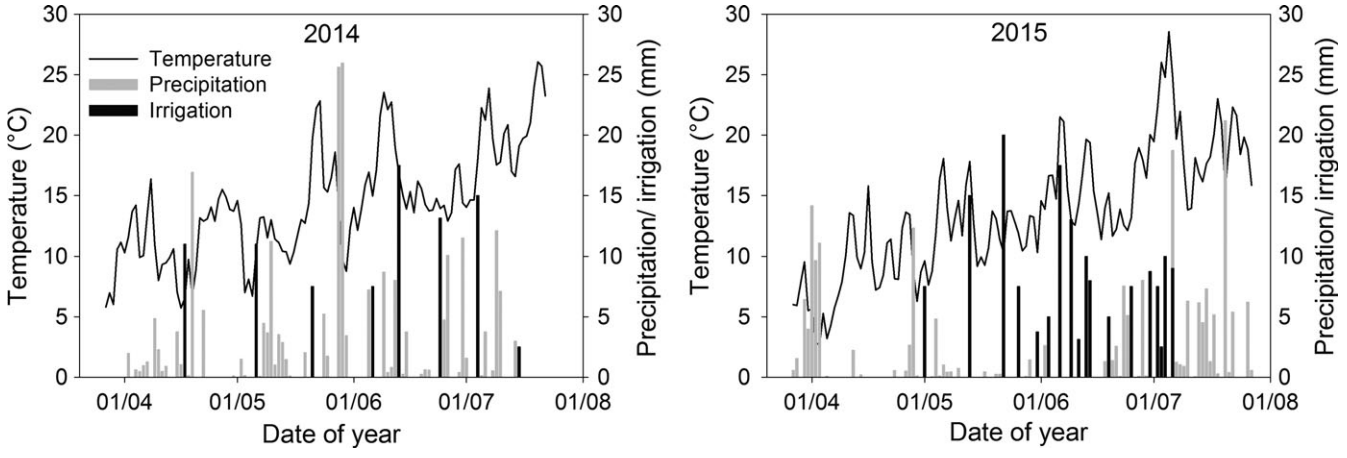

FIGURE 1 Course of daily mean temperature, precipitation, and irrigation over the main growing season

from LICOR) of subsamples of 25% of the harvests. In addition, the same subsample was used to determine biomass partitioning to leaf blades, ears, and stems after drying at 105°C. The rest of the sample was directly dried at 105°C followed by dry weight determination. Green area indices were determined on the basis of the measured green areas and dry weights. Leaf area index (LAI) was calculated as the mean over the three harvests and ear area index as the mean over the two final harvests. Residual leaf area index (RLAI) was computed by subtracting FLAI from LAI.

2.5 | Calculation of radiation-adjusted flag leaf and residual leaf area index

Irradiance (% of value at the top of canopy) that reached a certain canopy fraction (*I*) was calculated with the equation of Monsi and Saeki (2005):

$$I = e^{-k*\mathrm{GAI}}$$

where *k* is the extinction coefficient and GAI the cumulative green area index at the bottom of the considered canopy fraction. The extinction coefficient was assumed to be 0.53 prior and 0.58 from flowering stage onward according to Shearman, Sylvester-Bradley, Scott, and Foulkes (2005). The plant canopy was divided into three layers (ear, flag leaf, and residual leaves). Irradiance (relative irradiance with regard to the value at the top of the canopy) on a certain canopy layer was calculated by the mean of the value on top (i.e., the bottom of the overlying canopy layer) and on the bottom of the considered canopy layer. A value was calculated for the time before (minus ear) and after the flowering stage (plus ear) and both values were averaged. Radiation-adjusted flag leaf and residual leaf area indices were calculated by multiplying the irradiance on the flag leaf and residual leaf fraction with FLAI and RLAI, respectively.

2.6 | Measurement of aboveground biomass and N acquisition

Data of leaf blade, ear, stem, and total aboveground biomass at the milk-ripe stage were collected as described in 2.4. Dried plant material of leaf blades, ears, and stems was ground to a fine powder in a rotor mill (Brabender, Germany) and this material was analyzed for its N concentration (N conc) using an element analyzer (Leco TruSpec CNS, USA). N acquisition was calculated for each plant fraction by multiplying the N conc with the aboveground biomass. Total aboveground N acquisition was calculated by adding up the N acquisition of leaf blade, ear, and stem.

2.7 | Determination of flag leaf nitrate reductase activity (NRA)

Flag leaf NRA per gram fresh weight was measured with an in vitro assay according to Scheible, Lauerer, Schulze, Caboche, and Stitt (1997) with modifications. One hundred milligram of the liquid N_2 powdered material was thoroughly mixed with four volumes of ice-cold extraction buffer (100 mM HEPES-KOH (pH 7.5), 5 mM magnesium acetate, 1 mM EDTA, 10% (v/v) glycerol, 0.5% (w/v) BSA, 0.1% Triton X-100, 1% polyvinylpolypyrrolidone (PVPP), 5 μM $NaMoO_4$, 0.5 mM phenylmethylsulfonyl fluoride (PMSF), 5 mM DTT, 20 μM FAD, and 25 μM leupeptin).

Only the active state of NR was measured, so one volume of extract was mixed with five volumes of prewarmed (25.5°C) assay buffer in a heat block (100 mM HEPES-KOH, 6 mM KNO_3, 12 mM $MgOAc_2$, 0.6 mM NADH, 20 μM leupeptin, 12 μM FAD, 0.3 mM DTT, 6 μM $NaMoO_4$). After 5, 10, and 15 min at 25.5°C, respectively, the reaction was stopped by removing a 300 μl aliquot of the assay mixture and adding each aliquot to 25 μl 600 mM zinc acetate. To remove unreacted NADH, 75 μl 0.25 mM phenazine methosulfate was added and incubated for 15 min in the dark. Formed NO_2^- was determined colorimetrically as described by Scheible et al. (1997). Each sample was run in triplicates.

NRA per gram fresh weight was referred to m^2 ground area basis by using the dry weight/fresh weight ratio and FLB.

2.8 | Nitrate reductase gene expression analysis

Total wheat RNA of flag leaves from the second sampling at late flowering in 2015 (Table 2) was isolated using the innuPREP Plant RNA Kit (Analytik Jena, Germany) according to the manufacturer`s protocol with an additional DNase I digest (innuPREP DNase I-Mix (Analytik Jena, Germany)). Two hundred nanogram of total RNA was reverse transcribed via the innuSCRIPT reverse transcriptase kit (Analytik Jena, Germany). Quantitative reverse transcription PCR reactions were performed using the TOptical Thermocycler (Analytik Jena, Germany) and the innuMIX qPCR SyGreen MasterMix (Analytik Jena, Germany) with 1:50 cDNA dilutions. Nitrate reductase (*nia)* gene sequences on chromosomes 6AS, 6DS, and 7DS were identified via BLAST analysis of the International Wheat Genome Sequencing Consortium and Ensembl plants database. Primer sequences and gene accessions are listed in Table S1 in the supporting information. ADP-ribosylation factor and translation elongation factor 1 alpha were used as reference genes (Gimenez, Piston, & Atienza, 2011; Paolacci, Tanzarella, Porceddu, & Ciaffi, 2009). Primer efficiency was analyzed in cDNA dilution series and primer combinations with efficiencies between 95% and 105% were used. For calculation of relative fold changes and to test the statistical significance of the gene expression ratios, the **R**elative **E**xpression **S**oftware **T**ool 2009 (REST 2009) (Pfaffl, Horgan, & Dempfle, 2002) was used.

2.9 | Statistics

Each CO_2 × N combination was replicated three times. As an exception to this procedure for the measurement of NRA the samples in 2014 CUL180 ambient, CAN180 e[CO_2], and CAN320 e[CO_2] were tested in duplicates, and both CAN40 and CUL180 e[CO_2] as a singular probe due to tube breakage.

Wald *F*-tests were done with SAS (version 9.4) proc mixed using the following mixed model:

$$y = \mu + CO_2 + N + CO_2 \times N + R + e$$

where y is the dependent variable, μ the overall mean, CO_2 the CO_2 effect, N the N fertilizer effect, $CO_2 \times N$ the interaction effect, R the main plot error, and e the residual error. When sampling time was added as a third factor to the mixed model, *F*-tests were carried out as repeated measurements. In this case, sampling time was treated as a fixed effect and the UN(1) covariance model was used to model the correlation among samplings at different time points for the random main plot and residual error. The UN(1) model applies no covariance for sampling time, but allows different error variances for the different samplings. Least square difference (LSD) tests were carried out with SAS pro glimmix after removing the nonsignificant effects from the model. Mean values were regarded as significantly different if $p < .05$.

Each year was considered as an individual experiment. To take possible legacy effects with respect to soil mineral N availability into account, total soil mineral N in the 30 cm plough horizon was measured in all plots in March 2014 and 2015. Statistical analysis did not show a significant CO_2, N, and $CO_2 \times N$ effect on total soil mineral N as well as the NO_3^--N and NH_4^+-N content. Averaged over all CO_2 and N treatments the total soil mineral N was 14 kg N/ha in 2014 and 22 kg N/ha in 2015.

3 | RESULTS

3.1 | Pool size of mineral N in soil and wheat stem NO_3^- concentration

In 2015, NO_3^--N and NH_4^+-N were monitored over the whole growing season in the uppermost 30 cm soil profile of the NO_3^--based fertilization (CAN200) and the NH_4^+-based fertilization plots (UNI200). Statistical analysis showed neither a significant CO_2 effect nor an interaction with CO_2 for all tested parameters (Table 3). Therefore, mean values of NO_3^--N, NH_4^+-N, and total soil mineral N over both CO_2 treatments were used and are depicted in Figure 2. Statistical analysis comparing the time course of NO_3^--N as well as NH_4^+-N between the CAN200 and the UNI200 plots showed a significant N and N × sampling effect (Table 3). As depicted in Figure 2a soil NO_3^--N concentration of the CAN200 plots was higher compared to soil NH_4^+-N concentration over the whole growing season in 2015. In the UNI200 plots soil NH_4^+-N concentration was higher compared to soil NO_3^--N concentration over the growing season, except for one sampling at the end of April (Figure 2b). Averaged over the two CO_2 treatments and all samplings the soil NO_3^--N concentration was 21.3 kg/ha in the CAN200 plots and 9.0 kg/ha in the UNI200 plots. The soil NH_4^+-N concentration was 8.6 kg/ha in the CAN200 plots and 17.0 kg/ha in the UNI200 plots. However, no significant differences in total soil mineral N between the CAN200 and the UNI200 plots were observed (Table 3, Figure 2c).

Stem NO_3^- concentration was significantly lower in the UNI200 compared to the CAN200 treatment at two of four samplings in 2015 (Table 3, Figure 3). In contrast, no significant differences in stem NO_3^- concentration between the NO_3^--based CAN180 treatment and the CUL180 treatment were observed in 2014. Furthermore, CO_2 enrichment had no significant effect on stem NO_3^- concentration in both years.

3.2 | Leaf and ear growth

Table 4 presents the percentage effect of e[CO_2] and the statistics of the CO_2, N, and $CO_2 \times N$ effect on variables describing leaf and ear growth and Tables S2 and S3 the corresponding mean values. e[CO_2] significantly increased the following variables: flag leaf biomass per m^2 ground area, flag leaf area index, and radiation-adjusted flag leaf area index in all N treatments in both years; flag leaf number per m^2 ground area and ear area index in all N treatments in 2014; and flag leaf number per m^2 ground area and ear area index in all N treatments except under N deficiency (CAN35) in 2015. No significant CO_2 and $CO_2 \times N$ effect was observed for specific flag leaf

TABLE 3 Result of *F*-tests comparing the time course of stem NO_3^- concentration and of soil NO_3^--N, NH_4^+-N, and total mineral N concentration in the uppermost 30 cm soil layer. Results show stem NO_3^- concentration under two N (CAN180/CUL180) and two CO_2 treatments (ambient [CO_2]/e[CO_2]) in 2014 and soil NO_3^--N, NH_4^+-N, and total mineral N as well as stem NO_3^- concentration under two N (CAN200/UNI200) and two CO_2 treatments (ambient [CO_2]/ e[CO_2]) in 2015. Prior to analysis the data were log-transformed to comply with variance homogeneity

	2014	2015			
	Stem NO_3^- (mg/g)	Soil NO_3^--N (kg/ha)	Soil NH_4^+-N (kg/ha)	Soil total N (kg/ha)	Stem NO_3^- (mg/g)
CO_2	ns	ns	ns	ns	ns
N	ns	**	**	ns	**
$CO_2 \times N$	ns	ns	ns	ns	ns
Sampling (S)	**	**	**	**	**
$CO_2 \times S$	ns	ns	ns	ns	ns
$N \times S$	ns	**	*	ns	ns
$CO_2 \times N \times S$	ns	ns	ns	ns	ns

ns, not significant; *$p < .01$; **$p < .001$.

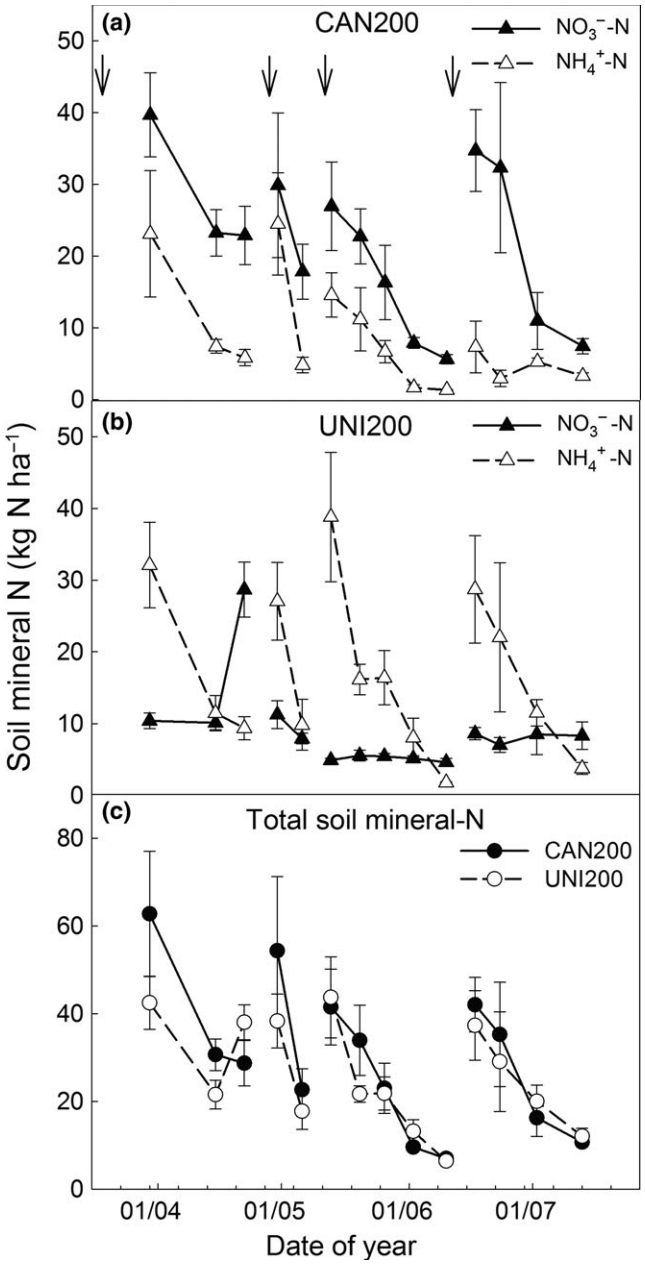

FIGURE 2 Time course of soil NO_3^--N and NH_4^+-N in the uppermost 30 cm soil profile of the CAN200 (a) and UNI200 treatment (b) during winter wheat growth. In (c), the amount of total soil mineral N in the CAN200 and UNI200 treatment is shown. Dates of N fertilization are indicated by arrows and data points around the N fertilizer applications are not interconnected. The data points represent mean values (± standard error of mean) over the two CO_2 treatments ($n = 6$)

weight, individual flag leaf area, residual leaf area index, and radiation-adjusted residual leaf area index.

3.3 | Flag leaf nitrate reductase activity and gene expression

Flag leaf nitrate reductase activity (NRA) referred to gram fresh weight was strongly influenced by N fertilization throughout all samplings in both 2014 and 2015 (Table 5). It was observed that NRA increased with increasing N fertilization (Figure 4), but neither a significant $CO_2 \times N$ interaction nor a significant CO_2 effect was observed in both years. Statistical analysis comparing flag leaf NRA between the two samplings within a particular year revealed no significant $CO_2 \times$ sampling and no $CO_2 \times N \times$ sampling interaction in both years. Despite the large temperature difference of 11°C between the first and second sampling in 2014 the measured NRA of the ambient and e[CO_2] treatments of each N fertilizer treatment showed no significant difference between the two samplings (Table 2, Figure 4). The calculation of flag leaf NRA per m^2 ground area revealed no e[CO_2] effect for the time before flowering in both years (Figure 5a,b). However, a higher NRA under e[CO_2] was observed at late flowering in 2015 (Figure 5c).

To test whether there are differences in flag leaf NRA between NO_3^-- and NH_4^+-based fertilization marginal N means (mean over both CO_2 treatments) between the CUL180 and the CAN180 treatment in 2014 as well as the UNI200 and the CAN200 treatment in 2015 were compared. No significant difference for the marginal N means of flag leaf NRA between the CUL180 and the CAN180 treatment was detected for both samplings in 2014 (Figure 4a). In 2015 on the other hand, the marginal N means of flag leaf NRA of the UNI200 and CAN200 treatments were similar at the first sampling, but were significantly lower for the UNI200 compared to the CAN200 treatment at the second sampling (Figure 4b). Furthermore, when referred to m^2 ground area significant differences in flag leaf NRA between the CAN200 and the UNI200 treatment were detected for both samplings in 2015 (Figure 5b,c), but no differences between the CAN180 and the CUL180 treatment were observed in 2014 (Figure 5a). Averaged over the two CO_2 treatments and both samplings flag leaf NRA referred to m^2 ground area of the CUL180 treatment was 98% of the NRA of the CAN180 treatment in 2014. In 2015, flag leaf NRA per m^2 ground area of the UNI200 treatment was 70% of the NRA of the CAN200 treatment.

Investigation of flag leaf NR (*nia*) gene expression of three NR genes localized on chromosome 6AS, 6DS, and 7DS revealed a considerable influence of N fertilization with significantly lower *nia* transcript levels for plants grown under CAN35 and UNI200 compared to plants grown under CAN200 and CAN320 (Fig. S1). However, no e[CO_2] effect on *nia* transcription was observed for any N fertilization treatments (Fig. S2).

3.4 | Total aboveground biomass and N acquisition

Aboveground biomass was increased by e[CO_2] with relative effects of 4 up to 20% in 2014 and 6 up to 24% in 2015, respectively (Figure 6a). Tissue N concentrations of stem, leaf, ear, and total plant were not significantly influenced by e[CO_2] in 2014 (Tables S5 and S6). In 2015, e[CO_2] significantly reduced N concentration of leaf (−15%) and total plant (−9%) of the CAN200 treatment as well as N concentration of leaf (−20%), ear (−11%), and total plant (−19%) of the UNI200 treatment. In 2014, N acquisition of the CAN180, CAN320, as well as CUL180 treatment was increased by e[CO_2]

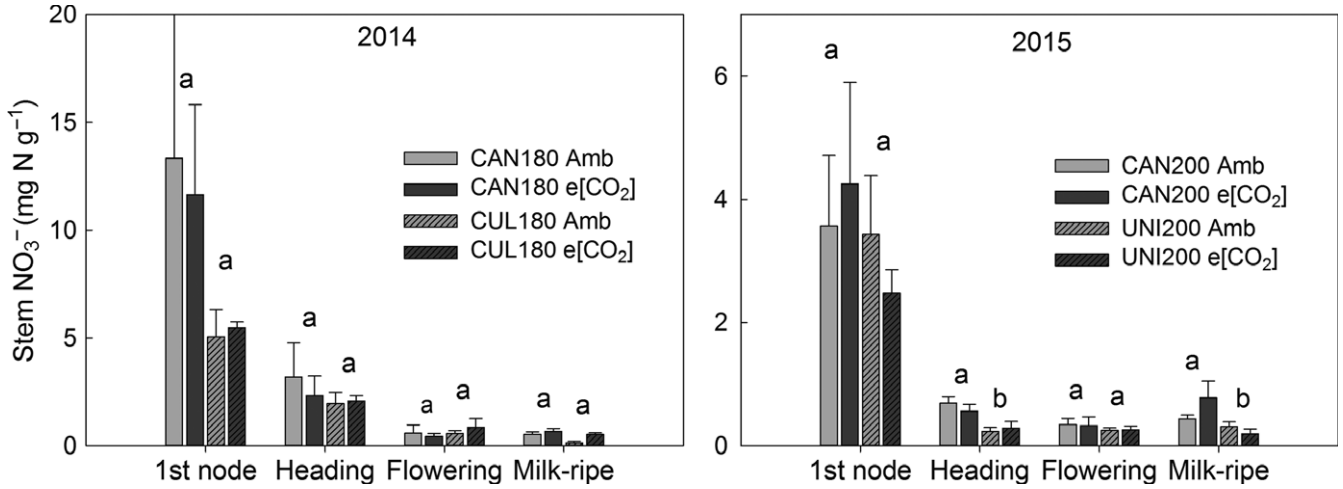

FIGURE 3 Effect of two CO_2 and two N treatments on stem NO_3^- concentration at four growing stages. Shown are the mean values (± standard error of mean; $n = 3$) for CAN180 and CUL180 in 2014 and for CAN200 and UNI200 in 2015. Different letters indicate significant differences among the marginal N means (mean over the two CO_2 treatments) separately for each growth stage. Note that one error bar of the sampling in 2014 goes beyond the diagram and that the scale of the *y*-axis differs between both diagrams

TABLE 4 Range of the percentage e[CO_2] effect (Δ) and *F*-test results of the CO_2, N and CO_2 × N effect on variables determining flag leaf growth and green area indices under all N treatments

	2014				2015			
	Δ (%)	CO_2	N	CO_2 × N	Δ (%)	CO_2	N	CO_2 × N
SFLW (g/m^2)	−3 to 6	ns	**	ns	−4 to −1	ns	***	ns
FLA (cm^2/leaf)	−4 to 19	ns	***	ns	6–14	ns	***	ns
FLN (m^{-2})	2–9	(*)	***	ns	−5 to 15	**	***	*
FLB (g/m^2)	6–29	*	***	ns	6–22	*	***	ns
FLAI (m^2/m^2)	4–24	*	***	ns	7–24	*	***	ns
RLAI (m^2/m^2)	−5 to 24	ns	***	ns	−4 to 8	ns	***	ns
EAI (m^2/m^2)	5–18	**	***	ns	−1 to 15	(*)	***	(*)
raFLAI (m^2/m^2)	2–18	*	***	ns	7–18	*	***	ns
raRLAI (m^2/m^2)	−19 to 11	ns	*	ns	−11 to −5	ns	***	ns

SFLW, specific flag leaf weight; FLA, individual flag leaf area; FLN, flag leaf number; FLB, flag leaf biomass; FLAI, flag leaf area index; RLAI, residual leaf area index; EAI, ear area index; raFLAI, radiation-adjusted flag leaf area index; raRLAI, radiation-adjusted residual leaf area index; ns, not significant; (*) $p < .1$; *$p < .05$; **$p < .01$; ***$p < .001$.

TABLE 5 *F*-test results for the effect of four N and two CO_2 treatments on NRA referred to gram fresh weight. Each sampling was analyzed separately and in addition both samplings of each year were subjected to a combined analysis. For the combined analysis of 2014 log-transformation was carried out to comply with variance homogeneity

	2014			2015		
	May 19th	May 22th	May 19th + May 22th	May 29th	June 15th	May 29th + June 15th
CO_2	ns	ns	ns	ns	ns	ns
N	**	**	**	**	**	**
CO_2 × N	ns	ns	ns	ns	ns	ns
Sampling (S)	–	–	*	–	–	*
CO_2 × S	–	–	ns	–	–	ns
N × S	–	–	ns	–	–	*
CO_2 × N × S	–	–	ns	–	–	ns

ns, not significant; *$p < .05$; **$p < .001$.

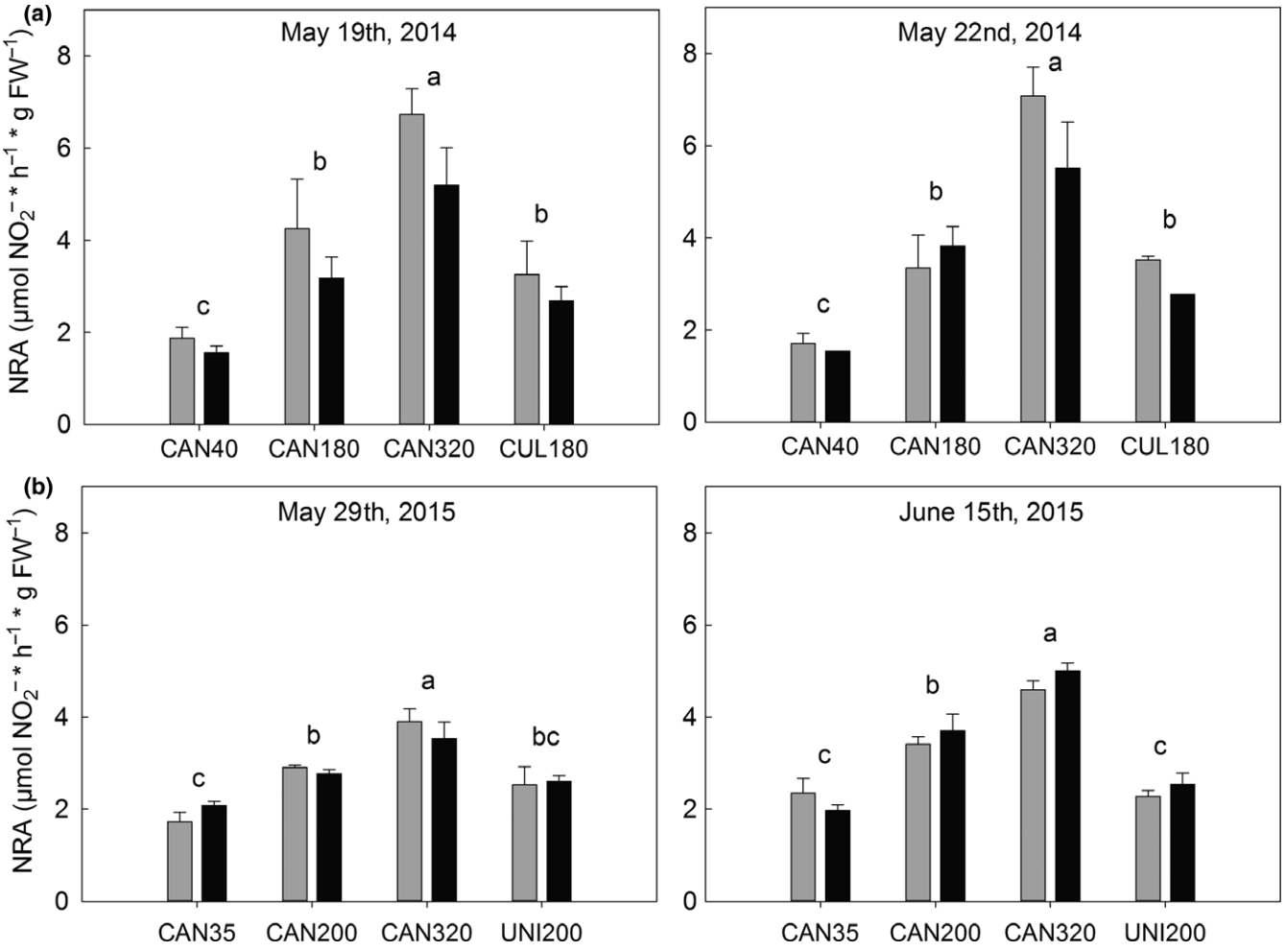

FIGURE 4 Effect of two CO_2 and four N treatments on flag leaf NRA referred to gram fresh weight. (a) Samplings in 2014 and (b) samplings in 2015 (mean± standard error of mean; for number of replicates see 2.9). Grey bars represent ambient [CO_2] and black bars e [CO_2]. Different letters indicate significant differences among the marginal means of the N treatments

with relative effects of 4 up to 13%, but this increase was not significant (Figure 6b). A significant CO_2 × N interaction was only observed in 2015. Here, e[CO_2] significantly increased N acquisition of the CAN200 and the CAN320 treatment by 14 and 16%, respectively. However, there was no e[CO_2] effect on N acquisition of the CAN35 and the UNI200 treatment (Figure 6b).

4 | DISCUSSION

A decline in NO_3^- assimilation and consequently lower protein concentrations in cereals under e[CO_2] would have unpredictable effects on future human and animal nutrition. Therefore, the effect of rising [CO_2] concentrations on N status of crops has been studied intensively (Ainsworth & Long, 2005; Taub & Wang, 2008). NO_3^- is the major plant-available N form in agricultural soils due to nitrification (Andrews et al., 2013; Subbarao et al., 2006) and consequently, the well-studied enzyme NR is of high interest with respect to its response to e[CO_2]. However, its regulation under these conditions is not completely understood as transcriptional regulation as well as posttranslational inhibition play important roles in the highly connected N and C metabolism (Stitt & Krapp, 1999). In this study it was tested whether NO_3^- assimilation is inhibited by e[CO_2] and whether an intensified growth and a higher N acquisition can be achieved with an NH_4^+-based fertilization in field-grown wheat.

4.1 | Leaf growth and estimation of flag leaf contribution to NO_3^- assimilation

The leaf canopy provides the main contribution to NO_3^- assimilation of crops (Andrews et al., 1992). In order to infer the e[CO_2] effect on the leaf canopy's NO_3^- assimilation the e[CO_2] effect on leaf growth has to be considered. In previous studies with wheat plants grown in pots with an artificial belowground environment, for instance, a restricted rooting volume or changed soil temperature as compared to the field (Arp, 1991; Long et al., 2005) was observed that specific leaf weight tended to be higher under e[CO_2] (Thilakarathne et al., 2013; Ziska et al., 2004). Furthermore, a slight increase in individual leaf area has been detected under restricted rooting volume (Seneweera & Conroy, 2005). In contrast, in the

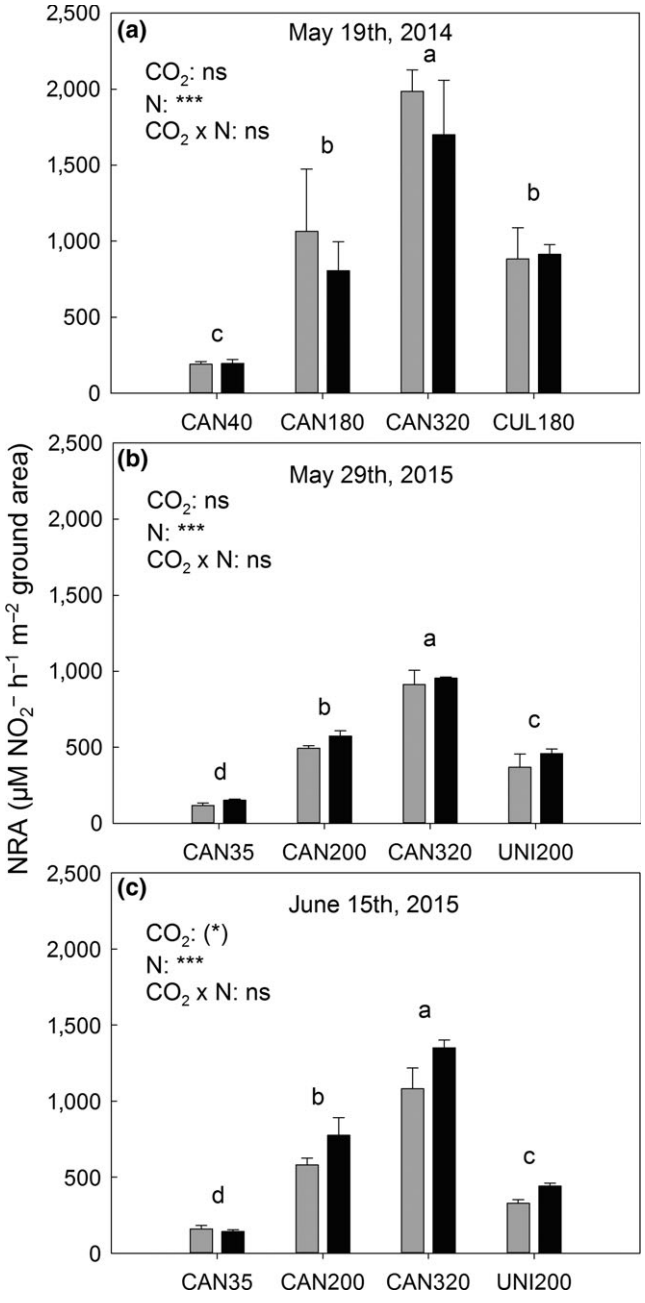

FIGURE 5 Effect of two CO_2 and four N treatments on flag leaf NRA referred to m^2 ground area. (a) Sampling before flowering in 2014, (b) sampling before flowering in 2015, (c) sampling at late flowering in 2015 (mean± standard error of mean; $n = 3$). Grey bars represent ambient [CO_2] and black bars e[CO_2]. *F*-test results are included in each diagram: ns: not significant; (*)$p < .10$; *$p < .05$; ***$p < .001$. Different letters indicate significant differences among the marginal means of the N treatments

present field study specific flag leaf weight as well as individual flag leaf area were not significantly altered by e[CO_2]. The observed significant increase in flag leaf biomass and flag leaf area per m^2 ground area under e[CO_2] resulted from a higher number of leaves as a result of an increased tiller number per plant. Higher tiller number per plant has also been found in another FACE study (Cai et al., 2016) as well as in a growth chamber study (Ziska et al., 2004).

NO_3^- assimilation and in particular nitrate reductase activity (NRA) depend on photosynthetic photon flux density (PPFD). The importance of flag leaves for NO_3^- assimilation was estimated on the basis of the PPFD distribution within the canopy because in this study only the NRA of the flag leaf was measured. Flag leaf area index accounted for only 28 up to 45% of the total leaf area index (Table S3) which might indicate a minor importance of the flag leaf for NO_3^- assimilation compared to the residual leaves. However, by taking into account that flag leaves were exposed to a higher PPFD, the radiation-adjusted flag leaf area index (raFLAI) was calculated. Based on this calculation flag leaves accounted for 38% at N deficiency (CAN40/35) up to 65% at N excess (CAN320) of the total leaf radiation-adjusted area index. Consequently, the flag leaf layer may constitute the major part of leaf NO_3^- assimilation under optimal and excess N fertilization. The importance of flag leaves is likely to increase until late grain filling as senescence proceeds from the bottom to the top of the canopy (Bertheloot, Martre, & Andrieu, 2008).

4.2 | Nitrate reductase activity and gene expression

In the present 2-year FACE experiment no significant inhibition of NRA under e[CO_2] was observed at four sampling dates. Therefore, the hypothesized decrease in NRA in wheat from other e[CO_2] studies conducted in hydroponic cultures (Bloom et al., 2002, 2010) cannot be supported with these results gained in this field experiment. Other FACE experiments with different plant species showed variable results regarding NRA. Natali, Sanudo-Wilhelmy, and Lerdau (2009) observed an inhibition of NRA in Loblolly pine (*Pinus taeda*), but no e[CO_2] effect for American sweetgum (*Liquidambar styraciflua*). Hu, Wang, Yang, Zhou, and Zhu (2006) found consistently higher NRA under e[CO_2] over the growing season for rice (*Oryza sativa*).

The NO_3^- assimilation is hypothesized to be inhibited under e[CO_2] due to a lower photorespiration rate and a subsequent lower supply of the reductant NADH for the NR caused by a decreased malate export from the chloroplast (Bloom, 2015a; Rachmilevitch et al., 2004). The malate valve represents an important player in the complex network between N and C metabolism and is involved in supplying energy in form of NADH for nitrate reduction (Scheibe, 2004). However, oxidation from triose phosphate sugars also increases cytosolic NADH availability and was long thought to be the ultimate energy source for NR as several intermediates and photosynthetic metabolites migrate from chloroplasts into the cytosol (Foyer et al., 2009; Kaiser et al., 2000). As cytosolic NADH concentration is generally estimated as very low it is uncertain to which amount the NADH for nitrate reduction is supplied by malate and to which amount from triose phosphate sugars originating from Calvin cycle. To address the dependency of NRA on photorespiration NRA was measured at moderate (16.7°C) and warm (27.6°C) temperature conditions before flowering in 2014. Between both temperatures no difference in NRA was observed. If this dependency would have been supported with this experiment, an inhibition of NRA by

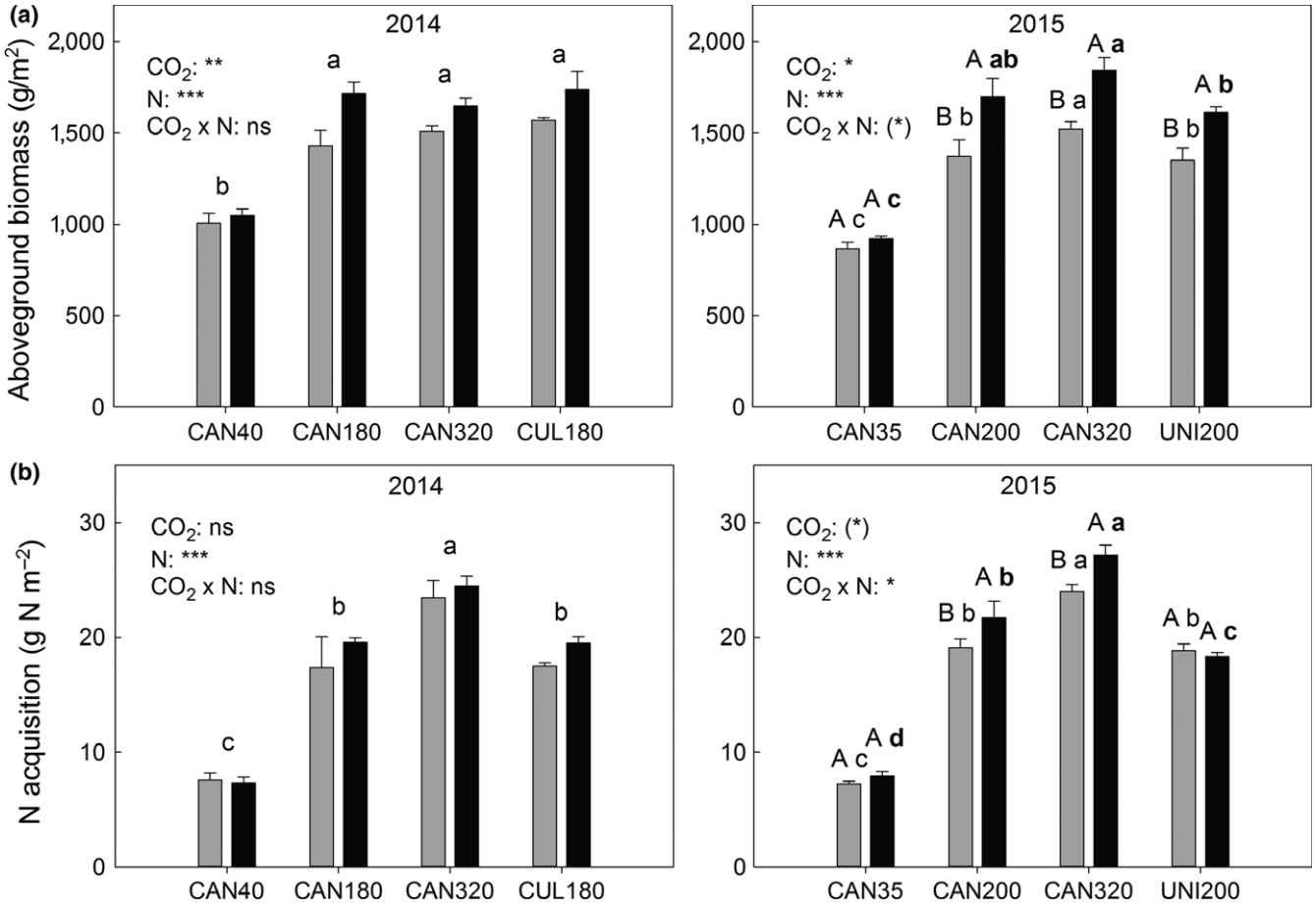

FIGURE 6 Effect of two CO_2 and four N treatments on aboveground biomass (a) and aboveground N acquisition (b) at the milk-ripe stage (mean± standard error of mean; $n = 3$). Grey bars represent ambient [CO_2] and black bars e[CO_2]. *F*-test results are included in each diagram: ns: not significant; (*)$p < .1$; *$p < .05$; **$p < .01$; ***$p < .001$. With no significant interaction from the *F*-test different lower case letters indicate significant differences among the marginal means of the N treatments. With significant interaction from the *F*-test different capital letters indicate significant differences for CO_2 means separate for each N treatment and different lower case letters show significant differences for N means separate for each CO_2 treatment (letters are in bold for e[CO_2])

e[CO_2] should be detectable at warm temperatures. This has been previously observed in a growth chamber study where e[CO_2] inhibited both photorespiration and NRA in wheat only at temperatures above 24°C (Jauregui et al., 2015). Nevertheless, the results of this study indicate no dependency of NRA on photorespiration in the field and suggest that rising temperatures will not induce or exacerbate inhibition of NO_3^- assimilation in wheat under future e[CO_2].

A FACE study indicated an inhibition of NO_3^- assimilation based on data of increased ratio of NO_3^- to total N concentration due to accumulation of unassimilated NO_3^- in leaf tissue (Bloom et al., 2014). In addition, less ^{15}N-enriched organic N and NO_3^- in leaf tissue under e[CO_2] was observed which the authors have claimed to result from declined NO_3^- assimilation relative to replenishment. Although no similar measurements were conducted in this study and vice versa, this study disagrees with the study of Bloom et al. (2014) because no declines in NRA as well as nitrate reductase (*nia)* transcript levels under e[CO_2] were observed. An explanation for the differing results might be that the experiment of Bloom et al. (2014) was conducted under subtropical climate and excess N fertilization with 350 kg N/ha. Under these conditions NRA might have been very high due to (i) the excess N fertilization as it was observed in this study and (ii) the theoretically high NADH supply from very high photorespiration rates owing to high daytime temperatures. Consequently, the described and hypothesized e[CO_2]-induced NADH shortage for NR due to reduced photorespiration (Bloom, 2015a; Bloom, 2015b) might therefore occur in the field only under extreme conditions that facilitate very high NRA, namely, very high photorespiration rates and excess N fertilization, but not under moderate climate and adequate N supply. Moreover, in the study of Bloom et al. (2014) e[CO_2] did not decrease N concentrations implying that despite inhibition of NO_3^- assimilation N acquisition of wheat was not strongly affected.

The regulation of the nitrate reductase (*nia)* transcript is rather complex but follows a light-dependent diurnal expression pattern and is generally positively influenced by increasing cellular NO_3^- and repressed by high glutamine levels (Stitt & Krapp, 1999). In this

study, the levels of *nia* transcript were significantly lower in the deficient NO_3^- (CAN35)- and optimal NH_4^+ (UNI200)-based fertilization treatments compared to the optimal (CAN200) and excessive (CAN320) NO_3^--based ones. These results support that increasing NO_3^- concentrations induced the *nia* transcription and suggest that an adaption to the lower NO_3^- status under N deficiency and NH_4^+-based fertilization took place. Regarding the e[CO_2] effect on flag leaf *nia* transcription Buchner et al. (2015) observed 1.6- to 1.8-fold higher *nia* transcript levels under e[CO_2] in spring wheat flag leaves at flowering. In contrast, in this study no significant differences in *nia* transcript levels were observed which is consistent with no e[CO_2] effect on flag leaf NRA. This discrepancy could be attributed to the different growing conditions between the two study sites. For example, in this study the irrigation was rigorously controlled, whereas in the study of Buchner et al. (2015) wheat was grown in dry-land agriculture.

4.3 | Establishment of an NH_4^+-based fertilization

In order to establish an NH_4^+-dominated fertilization, CULTAN fertilization was used in the 1st year and surface application consisting of a combination of urea with nitrification inhibitors in the 2nd year. Particularly in the first two growing stages, stem NO_3^- concentration was considerably higher in 2014 compared to 2015. This could indicate generally higher nitrification rates in spring 2014, which might be connected with the higher average temperature in April in 2014 (11.5°C) compared to 2015 (8.2°C). Net mineralization, which is another important NH_4^+ source, was estimated based on total N fertilizer applied and aboveground N acquisition in the N deficiency treatment (CAN40/35). This estimation resulted in no large difference between 2014 (35 kg N/ha) and 2015 (41 kg N/ha).

With CULTAN, depots containing high concentrations of NH_4^+ are injected into the soil next to the plants. The high NH_4^+ concentration of these depots is assumed to be toxic for microorganisms thus preventing nitrification and forcing plants to take up NH_4^+ (Petersen et al., 2004; Wetselaar et al., 1972). Consequently, rhizospere azidification by plant NH_4^+ uptake should further decrease nitrification because high nitrification rates occur at a neutrale soil pH (Suzuki et al., 1974). In this study in 2014, however, no differences in stem NO_3^- concentration as well as flag leaf NRA were observed, suggesting similar soil NO_3^--N supply for the CUL180 and CAN180 fertilization. Inadequate control of nitrification with CULTAN was also observed in another study because soil NO_3^--N content did not differ between CULTAN and surface spreading of ammonium sulfate (Deppe et al., 2016).

In contrast, in 2015, soil NO_3^--N concentration, stem NO_3^- concentration, flag leaf NRA, as well as flag leaf *nia* transcript levels were lower for plants grown under UNI200 compared to plants grown under CAN200, whereas total soil mineral N supply was similar in both N treatments. This result indicates lower NO_3^- but similar mineral N availability in the UNI200 compared to the CAN200 plots and suggests that nitrification was substantially controlled over the growing season in the UNI200 plots. Nevertheless, soil pH did not differ significantly between the CAN200 and UNI200 plots (data not shown), even if the soil pH decreased by 0.5 units from March until middle of June probably due to nitrification and/or plant NH_4^+ uptake. At the end of April 2015, a short-term increase in soil NO_3^--N occurred in the UNI200 plots which can be explained by the short half-live of nitrification inhibitors (Subbarao et al., 2006). Furthermore, unusual heavy rainfalls with 50 mm occurred between the end of March and the beginning of April. This may have caused leaching of nitrification inhibitors, which could have further decreased the inhibition efficiency. Apart from that, soil NO_3^--N concentration in the UNI200 plots remained constantly at a low level, but never fell to zero suggesting a base NO_3^--N level even under good nitrification control.

Averaged over CO_2 treatments and samplings, the soil NO_3^--N concentration in the UNI200 plots was only 40% of the soil NO_3^--N concentration in the CAN200 plots with similar soil mineral N supply for both N treatments. However, flag leaf NRA per m^2 ground area of plants grown with UNI200 fertilization was 70% compared to CAN200 fertilization. This indicates that wheat strongly favors NO_3^- over NH_4^+ assimilation even at high soil NH_4^+-N and low NO_3^--N supply. However, an ultimate proof which N form is preferred by the plant might provide the application of ^{15}N-labeled NO_3^- or NH_4^+ fertilizers and the subsequent tracing of the ^{15}N-labeled N compounds. In addition, the high NRA in the UNI200 treatment indicates that the largest portion of the urea applied in the UNI200 plots was nitrified.

Based on the preference of wheat to take up NO_3^- and the difficulty of keeping high NH_4^+-N concentrations in the soil, it can be predicted that the establishment of an agricultural system based on primary uptake of NH_4^+ as major N form is not readily manageable.

4.4 | Growth and N acquisition under NO_3^-- and NH_4^+-based fertilization

In this study aboveground biomass was significantly increased by e[CO_2] under optimal (CAN180/200) and excessive (CAN320) NO_3^--based fertilization as well as under CUL180 and NH_4^+-based fertilization (UNI200), but not under the severe N deficiency treatment (CAN40/35). Dependency on N availability and in particular declining growth stimulation by e[CO_2] under N deficiency has been reported for wheat (Wolf, 1996) and other species in growth chamber (Stitt & Krapp, 1999) and FACE studies (Ainsworth & Long, 2005). However, a NH_4^+-based fertilization did not enhance the stimulating effect of e[CO_2] on aboveground biomass any further compared to NO_3^--based fertilization as it was proposed by Bloom et al. (2002).

Previous meta-analyses that are primarily based on enclosure studies reported tissue N concentration decreases under e[CO_2] in wheat with an average of −16% for vegetative tissue (Cotrufo et al., 1998) and −10% for grain (Taub et al., 2008). However, previous FACE studies with wheat showed no decrease in N concentration of ear (Tausz-Posch et al., 2015) and only small decreases in stem and

leaf (Bloom et al., 2014; Tausz-Posch et al., 2015). In this FACE study under NO_3^--based fertilization, e[CO_2] did not significantly reduce stem and ear N concentration and the reduction in leaf N concentration was only moderate. For example, e[CO_2] decreased total plant tissue N concentration by only −5% in 2014 and −9% in 2015 in plants grown under optimal NO_3^--based fertilization. In addition to the milk-ripe stage, which is presented herein, four other growth stages analyzed in this study showed similarly moderate e[CO_2] effects on tissue N concentration (data not shown). It can therefore be concluded that the reduction in tissue N concentrations in wheat grown under e[CO_2] is generally lower in FACE compared to enclosure studies. In this study in plants grown under optimal NH_4^+-based fertilization (UNI200), e[CO_2] decreased total plant tissue N concentration by −19% and this reduction is considerably stronger compared to one observed in plants grown under NO_3^--based fertilization.

Due to the growth stimulation and only a slight decrease in tissue N concentration of plants grown under e[CO_2], the effect of e[CO_2] did not lead to a decrease but to an increase in aboveground N acquisition under NO_3^--based fertilization. This result is well reflected by the positive effects of e[CO_2] on NRA per m^2 ground area. The results with regard to the e[CO_2] effect on NRA, biomass, and aboveground N acquisition were similar between both years. Therefore, these results can be considered as representative at least for locations with similar conditions with regard to climate and soil. Higher N acquisition under e[CO_2] was also observed in other FACE experiments with NO_3^--based fertilization using the same wheat cultivar (Weigel & Manderscheid, 2012) as well as with other winter wheat cultivars (Cai et al., 2016; Han et al., 2015; Ma et al., 2007). Hence, a stimulation of NRA per m^2 ground area by e[CO_2] might have occurred in these studies. However, e[CO_2] did not increase N acquisition with an optimal NH_4^+-based fertilization (UNI200) and this result disagrees with the results of hydroponic experiments of Bloom et al. (2002) and Carlisle et al. (2012). Besides the physiological differences in terms of plant NO_3^- and NH_4^+ acquisition, it is important to consider the differences between a NO_3^-- and NH_4^+-based fertilization in terms of N losses to the environment (Masclaux-Daubresse et al., 2010). In this study under all N treatments but excess fertilization (CAN320), the plants acquired about 90% of the soil mineral N deriving from fertilization and mineralization. This indicates generally high nitrogen use efficiency in our study as well as no difference between the N fertilizer forms (CAN180/200 vs. CUL180/UNI200) in terms of N losses to the environment.

In conclusion, our results suggest that NO_3^--based fertilization is superior to an NH_4^+-based one under e[CO_2] for field-grown wheat. Therefore, a change from NO_3^-- to NH_4^+-based fertilization might not be beneficial under future e[CO_2]. Furthermore, our results suggest that an inhibition of NO_3^- assimilation by e[CO_2], as postulated in prior research, is not the reason for the decrease in tissue N concentration under e[CO_2] and that the reduction in e[CO_2] on tissue N concentration in wheat is much smaller in field studies with FACE compared to enclosure studies.

ACKNOWLEDGEMENTS

We thank P. Braunisch, A. Fuehrer, A. Kremling, E. Schummer R. Staudte, and the experimental station of the Friedrich-Loeffler Institute for excellent technical assistance with the FACE experiment. We are grateful to H. Reuper and the students of the Institute for Plant Biology of the Technische Universität Braunschweig for their support in the NRA assay. Dr. H. Hahn and the company SKW Piesteritz are greatly acknowledged for the provision of Alzon M+ and their helpful hints. We thank the reviewers for their valuable comments and helpful suggestions to improve the original manuscript. This work was partly funded by the German Science Foundation (DFG).

CONFLICT OF INTEREST

None of the authors has any conflict of interest to declare.

REFERENCES

Ainsworth, E. A., & Long, S. P. (2005). What have we learned from 15 years of free-air CO_2 enrichment (FACE)? A meta-analytic review of the responses of photosynthesis, canopy properties and plant production to rising CO_2. *New Phytologist*, *165*, 351–371.

Andrews, M., Morton, J. D., Lieffering, M., & Bisset, L. (1992). The partitioning of nitrate assimilation between root and shoot of a range of temperate cereals and pasture grasses. *Annals of Botany*, *70*, 271–276.

Andrews, M., Raven, J. A., & Lea, P. J. (2013). Do plants need nitrate? The mechanisms by which nitrogen form affects plants. *Annals of Applied Biology*, *163*, 174–199.

Arp, W. J. (1991). Effects of source-sink relations on photosynthetic acclimation to elevated CO_2. *Plant Cell and Environment*, *14*, 869–875.

Bertheloot, J., Martre, P., & Andrieu, B. (2008). Dynamics of light and nitrogen distribution during grain filling within wheat canopy. *Plant Physiology*, *148*, 1707–1720.

Bloom, A. J. (2015a). The increasing importance of distinguishing among plant nitrogen sources. *Current Opinion in Plant Biology*, *25*, 10–16.

Bloom, A. J. (2015b). Photorespiration and nitrate assimilation: A major intersection between plant carbon and nitrogen. *Photosynthesis Research*, *123*, 117–128.

Bloom, A. J., Burger, M., Kimball, B. A., & Pinter, P. J. Jr (2014). Nitrate assimilation is inhibited by elevated CO_2 in field-grown wheat. *Nature Climate Change*, *4*, 477–480.

Bloom, A. J., Burger, M., Rubio-Asensio, J. S., & Cousins, A. B. (2010). Carbon dioxide enrichment inhibits nitrate assimilation in wheat and Arabidopsis. *Science*, *328*, 899–903.

Bloom, A. J., Rubio-Asensio, J. S., Randall, L., Rachmilevitch, S., Cousins, A. B., & Carlisle, E. A. (2012). CO_2 enrichment inhibits shoot nitrate assimilation in C_3 but not C_4 plants and slows growth under nitrate in C_3 plants. *Ecology*, *93*, 355–367.

Bloom, A. J., Smart, D. R., Nguyen, D. T., & Searles, P. S. (2002). Nitrogen assimilation and growth of wheat under elevated carbon dioxide. *Proceedings of the National Academy of Sciences of the United States of America*, *99*, 1730–1735.

Buchner, P., Tausz, M., Ford, R., Leo, A., Fitzgerald, G. J., Hawkesford, M. J., & Tausz-Posch, S. (2015). Expression patterns of C- and N-metabolism related genes in wheat are changed during senescence under elevated CO_2 in dry-land agriculture. *Plant Science*, *236*, 239–249.

Cai, C., Yin, X., He, S., Jiang, W., Si, C., Struik, P. C., ... Pan, G. (2016). Responses of wheat and rice to factorial combinations of ambient and elevated CO_2 and temperature in FACE experiments. *Global Change Biology*, *22*, 856–874.

Carlisle, E., Myers, S., Raboy, V., & Bloom, A. (2012). The effects of inorganic nitrogen form and CO_2 concentration on wheat yield and nutrient accumulation and distribution. *Frontiers in Plant Science*, *3*, 1–13.

Cotrufo, M. F., Ineson, P., & Scott, A. (1998). Elevated CO_2 reduces the nitrogen concentration of plant tissues. *Global Change Biology*, *4*, 43–54.

Deppe, M., Well, R., Kuecke, M., Fuss, R., Giesemann, A., & Flessa, H. (2016). Impact of CULTAN fertilization with ammonium sulfate on field emissions of nitrous oxide. *Agriculture Ecosystems and Environment*, *219*, 138–151.

Foyer, C. H., Bloom, A. J., Queval, G., & Noctor, G. (2009). Photorespiratory metabolism: Genes, mutants, energetics, and redox signaling. *Annual Review of Plant Biology*, *60*, 455–484.

Gimenez, M. J., Piston, F., & Atienza, S. G. (2011). Identification of suitable reference genes for normalization of qPCR data in comparative transcriptomics analyses in the Triticeae. *Planta*, *233*, 163–173.

Han, X., Hao, X., Lam, S. K., Wang, H., Li, Y., Wheeler, T., ... Lin, E. (2015). Yield and nitrogen accumulation and partitioning in winter wheat under elevated CO_2: A 3-year free-air CO_2 enrichment experiment. *Agriculture Ecosystems and Environment*, *209*, 132–137.

Hu, J., Wang, Y., Yang, L., Zhou, J., & Zhu, J. (2006). Effect of free-air CO_2 enrichment (FACE) on leaf nitrate reductase activity of *Oryza sativa* L. cultivar Wuxianjing 14. *Ying Yong Sheng Tai Xue Bao*, *17*, 2179–2184.

IPCC (2013). Climate Change 2013: The physical science basis. In T. F. Stocker, D. Qin, G.-K. Plattner, M. Tignor, S. K. Allen, J. Boschung, A. Nauels, Y. Xia, V. Bex & P. M. Midgley (Eds.), *Contribution of Working Group I to the Fifth Assessment Report of the Intergovernmental Panel on Climate Change*. Cambridge, UK: Cambridge University Press, 1535 pp.

Jauregui, I., Aroca, R., Garnica, M., Zamarreno, A. M., Garcia-Mina, J. M., Serret, M. D., ... Aranjuelo, I. (2015). Nitrogen assimilation and transpiration: Key processes conditioning responsiveness of wheat to elevated CO_2 and temperature. *Physiologia Plantarum*, *155*, 338–354.

Kaiser, W. M., Kandlbinder, A., Stoimenova, M., & Glaab, J. (2000). Discrepancy between nitrate reduction rates in intact leaves and nitrate reductase activity in leaf extracts: What limits nitrate reduction in situ? *Planta*, *210*, 801–807.

Lewin, K. F., Hendrey, G. R., & Kolber, Z. (1992). BROOKHAVEN Brookhaven National Laboratory free-air carbon-dioxide enrichment facility. *Critical Reviews in Plant Sciences*, *11*, 135–141.

Long, S. P., Ainsworth, E. A., Leakey, A. D. B., & Morgan, P. B. (2005). Global food insecurity. Treatment of major food crops with elevated carbon dioxide or ozone under large-scale fully open-air conditions suggests recent models may have overestimated future yields. *Philosophical Transactions of the Royal Society B-Biological Sciences*, *360*, 2011–2020.

Ma, L., Shan, J., & Yan, X. Y. (2015). Nitrite behavior accounts for the nitrous oxide peaks following fertilization in a fluvo-aquic soil. *Biology and Fertility of Soils*, *51*, 563–572.

Ma, H.-L., Zhu, H.-G., Liu, G., Xie, Z.-B., Wang, Y.-L., Yang, L.-X., & Zeng, Q. (2007). Availability of soil nitrogen and phosphorus in a typical rice-wheat rotation system under elevated atmospheric CO_2. *Field Crops Research*, *100*, 44–51.

Masclaux-Daubresse, C., Daniel-Vedele, F., Dechorgnat, J., Chardon, F., Gaufichon, L., & Suzuki, A. (2010). Nitrogen uptake, assimilation and remobilization in plants: Challenges for sustainable and productive agriculture. *Annals of Botany*, *105*, 1141–1157.

Monsi, M., & Saeki, T. (2005). On the factor light in plant communities and its importance for matter production. *Annals of Botany*, *95*, 549–567.

Myers, S. S., Zanobetti, A., Kloog, I., Huybers, P., Leakey, A. D. B., Bloom, A. J., ... Usui, Y. (2014). Increasing CO_2 threatens human nutrition. *Nature*, *510*, 139–142.

Natali, S. M., Sanudo-Wilhelmy, S. A., & Lerdau, M. T. (2009). Effects of elevated carbon dioxide and nitrogen fertilization on nitrate reductase activity in sweetgum and loblolly pine trees in two temperate forests. *Plant and Soil*, *314*, 197–210.

Pacholski, A., Manderscheid, R., & Weigel, H. J. (2015). Effects of free air CO_2 enrichment on root growth of barley, sugar beet and wheat grown in a rotation under different nitrogen supply. *European Journal of Agronomy*, *63*, 36–46.

Padgett, P. E., & Leonard, R. T. (1993). Contamination of ammonium-based nutrient solutions by nitrifying organisms and the conversion of ammonium to nitrate. *Plant Physiology*, *101*, 141–146.

Paolacci, A. R., Tanzarella, O. A., Porceddu, E., & Ciaffi, M. (2009). Identification and validation of reference genes for quantitative RT-PCR normalization in wheat. *BMC Molecular Biology*, *10*, 11.

Petersen, J., Hansen, B., & Sorensen, P. (2004). Nitrification of N-15-ammonium sulphate and crop recovery of N-15-labelled ammonium nitrates injected in bands. *European Journal of Agronomy*, *21*, 81–92.

Pfaffl, M. W., Horgan, G. W., & Dempfle, L. (2002). Relative expression software tool (REST) for group-wise comparison and statistical analysis of relative expression results in real-time PCR. *Nucleic Acids Research*, *30*, e36.

Pleijel, H., & Uddling, J. (2012). Yield vs. Quality trade-offs for wheat in response to carbon dioxide and ozone. *Global Change Biology*, *18*, 596–605.

Rachmilevitch, S., Cousins, A. B., & Bloom, A. J. (2004). Nitrate assimilation in plant shoots depends on photorespiration. *Proceedings of the National Academy of Sciences of the United States of America*, *101*, 11506–11510.

Scheibe, R. (2004). Malate valves to balance cellular energy supply. *Physiologia Plantarum*, *120*, 21–26.

Scheible, W. R., Lauerer, M., Schulze, E. D., Caboche, M., & Stitt, M. (1997). Accumulation of nitrate in the shoot acts as a signal to regulate shoot-root allocation in tobacco. *Plant Journal*, *11*, 671–691.

Seneweera, S. P., & Conroy, J. P. (2005). Enhanced leaf elongation rates of wheat at elevated CO_2: Is it related to carbon and nitrogen dynamics within the growing leaf blade? *Environmental and Experimental Botany*, *54*, 174–181.

Shearman, V. J., Sylvester-Bradley, R., Scott, R. K., & Foulkes, M. J. (2005). Physiological processes associated with wheat yield progress in the UK. *Crop Science*, *45*, 175–185.

Sinclair, T. R., Pinter, P. J., Kimball, B. A., Adamsen, F. J., Lamorte, R. L., Wall, G. W., ... Matthias, A. (2000). Leaf nitrogen concentration of wheat subjected to elevated CO_2 and either water or N deficits. *Agriculture Ecosystems and Environment*, *79*, 53–60.

Stitt, M., & Krapp, A. (1999). The interaction between elevated carbon dioxide and nitrogen nutrition: The physiological and molecular background. *Plant Cell and Environment*, *22*, 583–621.

Subbarao, G. V., Ito, O., Sahrawat, K. L., Berry, W. L., Nakahara, K., Ishikawa, T., ... Rao, I. M. (2006). Scope and strategies for regulation of nitrification in agricultural systems-challenges and opportunities. *Critical Reviews in Plant Sciences*, *25*, 303–335.

Suzuki, I., Dular, U., & Kwok, S. C. (1974). Ammonia or ammonium ion as substrate for oxidation by nitrosomonas-europaea cells and extracts. *Journal of Bacteriology*, *120*, 556–558.

Taniguchi, M., & Miyake, H. (2012). Redox-shuttling between chloroplast and cytosol: Integration of intra-chloroplast and extra-chloroplast metabolism. *Current Opinion in Plant Biology*, *15*, 252–260.

Taub, D. R., Miller, B., & Allen, H. (2008). Effects of elevated CO_2 on the protein concentration of food crops: A meta-analysis. *Global Change Biology*, *14*, 565–575.

Taub, D. R., & Wang, X. (2008). Why are nitrogen concentrations in plant tissues lower under elevated CO_2? A critical examination of the hypotheses. *Journal of Integrative Plant Biology*, *50*, 1365–1374.

Tausz-Posch, S., Dempsey, R. W., Seneweera, S., Norton, R. M., Fitzgerald, G., & Tausz, M. (2015). Does a freely tillering wheat cultivar

benefit more from elevated CO_2 than a restricted tillering cultivar in a water-limited environment? *European Journal of Agronomy*, *64*, 21–28.

Thilakarathne, C. L., Tausz-Posch, S., Cane, K., Norton, R. M., Tausz, M., & Seneweera, S. (2013). Intraspecific variation in growth and yield response to elevated CO_2 in wheat depends on the differences of leaf mass per unit area. *Functional Plant Biology*, *40*, 185–194.

Weigel, H.-J., & Manderscheid, R. (2012). Crop growth responses to free air CO_2 enrichment and nitrogen fertilization: Rotating barley, ryegrass, sugar beet and wheat. *European Journal of Agronomy*, *43*, 97–107.

Wetselaar, R., Passioura, J. B., & Singh, B. R. (1972). Consequences of banding nitrogen fertilizers in soil. 1. Effects on nitrification. *Plant and Soil*, *36*, 159–175.

Wieser, H., Manderscheid, R., Erbs, M., & Weigel, H. J. (2008). Effects of elevated atmospheric CO_2 concentrations on the quantitative protein composition of wheat grain. *Journal of Agricultural and Food Chemistry*, *56*, 6531–6535.

Wolf, J. (1996). Effects of nutrient supply (NPK) on spring wheat response to elevated atmospheric CO_2. *Plant and Soil*, *185*, 113–123.

Ziska, L. H., Morris, C. F., & Goins, E. W. (2004). Quantitative and qualitative evaluation of selected wheat varieties released since 1903 to increasing atmospheric carbon dioxide: Can yield sensitivity to carbon dioxide be a factor in wheat performance? *Global Change Biology*, *10*, 1810–1819.

SUPPORTING INFORMATION

Additional Supporting Information may be found online in the supporting information tab for this article.

How to cite this article: Dier M, Meinen R, Erbs M, et al. Effects of free air carbon dioxide enrichment (FACE) on nitrogen assimilation and growth of winter wheat under nitrate and ammonium fertilization. *Glob Change Biol*. 2018;24:e40–e54. https://doi.org/10.1111/gcb.13819